Supplemental material

Importance of hydrophilic hydration and intramolecular interactions in the thermodynamics of helix-coil transition and helix-helix assembly in a deca-alanine peptide

Dheeraj S. Tomar,[1] Valéry Weber,[2] B. Montgomery Pettitt,[3] and D. Asthagiri[4,3,*]

[1]*Department of Chemical and Biomolecular Engineering, Johns Hopkins University, Baltimore, MD 21218*

[2]*IBM Research, Zurich, CH-8803 Rüschlikon, Switzerland*

[3]*Sealy Center for Structural Biology and Molecular Biophysics, Department of Biochemistry and Molecular Biology, University of Texas Medical Branch, Galveston, TX 77555*

[4]*Department of Chemical and Biomolecular Engineering, Rice University, Houston, TX*

[*] Dilip.Asthagiri@rice.edu

S.I. METHODS

The methods closely follow our earlier study [1]. For completeness these together with key changes are presented here.

The simulations were performed at a temperature of 298.15 K and a pressure of 1 bar using, respectively, a Langevin thermostat and a Langevin barostat [2]. The decay constant of the thermostat was 1 ps^{-1}. The barostat piston period was 200 fs and the decay time was 100 fs. The SHAKE algorithm [3] was used to constrain the geometry of water molecules. The equations of motion were propagated using the Verlet algorithm with a time step of 2.0 fs. Lennard-Jones interactions were terminated at 10.43 Å by smoothly switching to zero starting at 9.43 Å. Electrostatic interactions were treated with the particle mesh Ewald method with a grid spacing of 0.5 Å.

For analyzing helix-coil transition, we studied the hydration of an isolated helix, the extended coil state C_0, and the coil states $\{C_1, \ldots, C_9\}$, obtained from the forced-unfolding in vacuum (Sec. S.II). For the analyzing the pairing of helices, we considered helix-pairs with helix axes parallel to each other. Helix dipoles with parallel and antiparallel orientations were considered. For calculating the hydration contribution to the potential of mean force $W_{solv}(r)$, where r is the separation between the helix axes, the helix-pair was treated as one unit (molecule). Thus

$$W_{solv}(r) = \mu^{\mathrm{ex}}(r) - 2\mu^{\mathrm{ex}} \tag{S.1}$$

where $\mu^{\mathrm{ex}}(r)$ is the hydration free energy of the helix-pair separated by a distance r and μ^{ex} is the hydration free energy of the isolated helix.

A. Chemistry and packing contributions

We apply atom-centered fields to carve out a molecular cavity in the liquid (Fig. 1, main text). We use the Tcl-interface to NAMD [4] to impose forces on the solvent due to the field. The functional form of the field was as before (Eq. 4b, Ref. 5):

$$\phi_\lambda(r) = 4a\left[\left(\frac{b}{r-\lambda+\sqrt[6]{2}b}\right)^{12} - \left(\frac{b}{r-\lambda+\sqrt[6]{2}b}\right)^{6}\right] + a\ , \tag{S.2}$$

where $a = 0.155$ kcal/mol and $b = 3.1655$ Å are positive constants and $(r < \lambda)$, and $\phi_\lambda(r) = 0$ for $r \geq \lambda$.

To build the field to its eventual range of $\lambda = 5$ Å, we progressively apply the field, and for every unit Å increment in the range, we compute the work done in applying the field using a five-point Gauss-Legendre quadrature [6]. Five Gauss-points $\left[0, \pm(1/3)\sqrt{5-2\sqrt{10/7}}, \pm(1/3)\sqrt{5+2\sqrt{10/7}}\right]$ are chosen for each unit Å. At each Gauss-point, the system was simulated for 1 ns and the (force) data from the last 0.75 ns used for analysis. (Excluding more data did not change the numerical value significantly, indicating good convergence.) Error analysis and error propagation was performed as before [5]: the standard error of the mean force was obtained using the Friedberg-Cameron algorithm [7, 8] and in adding multiple quantities, the errors were propagated using standard variance-addition rules.

The starting configuration for each λ point is obtained from the ending configuration of the previous point in the chain of states. For the packing contributions, a total of 25 Gauss points span $\lambda \in [0, 5]$. For the chemistry contribution, since solvent never enters $\lambda < 2.5$ Å, we simulate $\lambda \in [2, 5]$ for a total of 15 Gauss points.

For the helix and C_0 states alone, we repeated the above procedure for chemistry and packing calculations four times, ensuring that the solvent coordinates are different each time. The average and associated statistical uncertainties of this procedure are indicated in Table 1 (main text).

B. Long-range contribution

For $\lambda = 5$ Å, the conditional solute-solvent binding energy distribution $P(\varepsilon|\phi_\lambda)$ is Gaussian, as is the solute-solvent binding energy distribution $P^{(0)}(\varepsilon|\phi_\lambda)$ with solute and solvent thermally uncoupled. For this condition, it is well-known that $\mu^{\text{ex}}[P(\varepsilon|\phi_\lambda)]$ and $\mu^{\text{ex}}[P^{(0)}(\varepsilon|\phi_\lambda)]$ are equal [9], where

$$\begin{aligned} \mu^{\text{ex}}[P(\varepsilon|\phi_\lambda)] &= \langle\varepsilon\rangle + \frac{\beta}{2}\sigma^2 \\ \mu^{\text{ex}}[P^{(0)}(\varepsilon|\phi_\lambda)] &= \langle\varepsilon\rangle_0 - \frac{\beta}{2}\sigma^2 \,. \end{aligned} \tag{S.3}$$

In the above equations, $\langle\varepsilon\rangle$ and $\langle\varepsilon\rangle_0$ are the mean binding energies in the coupled and uncoupled ensembles, respectively, and σ^2 is the variance of the distribution, the same for both $P(\varepsilon|\phi_\lambda)$ and $P^{(0)}(\varepsilon|\phi_\lambda)$. Since calculations with $P^{(0)}(\varepsilon|\phi_\lambda)$ are typically more robust [10] numerically, the long-range contributions were obtained using the particle insertion

procedure. But we note that as before [1] test calculations with $P(\varepsilon|\phi_\lambda)$ leads to the same long-range contribution as the insertion procedure within statistical uncertainties of the either calculation.

All calculations of long-range interactions were preceded by a 1 ns equilibration of the appropriate cavity. The starting configuration for the $\lambda = 5$ Å simulation was obtained from the endpoint of the Gauss-Legendre procedure for the packing calculation. For helix and C_0 states, we performed test particle insertion in 40,000 frames collected over 40 ns of simulation. For the remaining coil conformations $\{C_1, \ldots, C_9\}$, we performed insertions in 2,000 frames collected over 2 ns. For the helix-pairs, test-particle insertions were performed in 10,000 frames collected from 10 ns of production.

Calculation of ε for a given solvent configuration is as follows. We calculated the potential energy, U_w, of the solvent configuration alone. (This was standardly performed in NAMD by running the code for zero time steps of dynamics.) Likewise, the potential energy of the solute plus solvent configuration, U_{sw}, and the potential energy of the solute, U_s, was obtained. Then $\varepsilon = U_{sw} - U_w - U_s$. The treatment of long-range interactions was exactly as that involved during dynamics. To characterize $P(\varepsilon|\phi_\lambda)$, the PairInteraction module in NAMD provided an easier way to calculate the binding energies.

Electrostatic self-interaction corrections were obtained following Hummer et al. [11, 12]. These turn out to be important for the helix state and for the helix pairs. The correction for the helix was about -0.5 kcal/mole and for the coil it was an order of magnitude lower. For the helix-pair with parallel arrangement of helix-dipoles, the self-interaction correction reached a minimum value of -2 kcal/mol for $r = 7.5$ Å. For the antiparallel helices, the minimum value of the correction is -0.3 kcal/mol occurring at $r = 14.5$ Å.

S.II. SAMPLING UNFOLDED STATES

We used the adaptive-bias force (ABF) approach [16, 17] to unfold the helix in vacuum and this calculation additional gave the free energy of unfolding in vacuum. We closely followed the ABF documentation (within NAMD) in performing the simulation. The distance, ξ, between the terminal carbon atoms — methyl-carbon of the acetyl group and the methyl-carbon of the n-methyl-amide group — defined the reaction coordinate. ξ was varied between 16 Å (helix) and 36 Å (extended coil).

Calculations were run for 100 ns, of which we used the last 50 ns for analysis. The temperature was maintained at 298 K using a Langevin thermostat with a friction coefficient of 10 ps^{-1}. The equations of motion were integrated using a time-step of 1 fs. The biasing forces were binned in windows of width 0.1 Å along ξ. The biasing force (in each bin) is adaptively updated such that at convergence its effect is to cancel the force due to underlying free energy surface (the quantity of interest). From the converged average-force-*vs*-ξ data, we then obtained the potential of mean force, $W(\xi)$, by integration (Fig. S1). To assess the role of forcefield, we performed corresponding simulations with the recently re-optimized c36 [18] variant of the CHARMM forcefield.

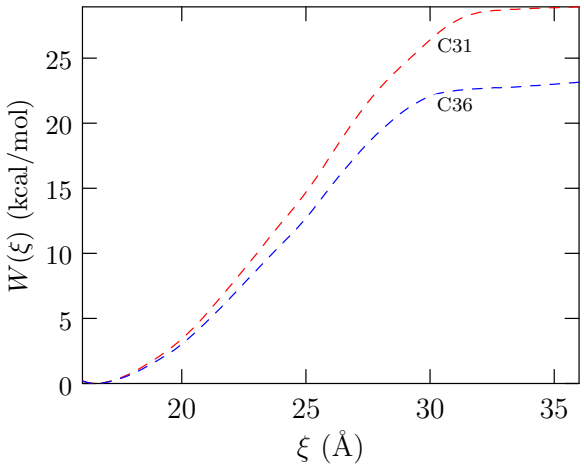

FIG. S1. The sensitivity of the potential of mean force for unfolding a deca-alanine helix in vacuum to slightly different variants of the CHARMM forcefield. The C_0 ($\xi = 36.8$ Å, $\Delta\mu^{\rm ex} \approx -7$ kcal/mol) and C_7 ($\xi = 34.0$ Å, $\Delta\mu^{\rm ex} \approx -14$ kcal/mol) coil states have roughly the same $W(\xi)$. Notice that the c36 forcefield improves the balance towards the coil state.

S.III. ENTHALPIC AND ENTROPIC CONTRIBUTIONS TO HYDRATION

From the Euler relation for the pure solvent and the solvent with one added solute, we can show that the excess entropy of hydration is

$$\begin{aligned} Ts^{\rm ex} &= E^{\rm ex} - kT^2\alpha_p + p(\langle V^{\rm ex}\rangle + kT\kappa_T) - \mu^{\rm ex} \\ &\approx E_{sw} + E_{reorg} - \mu^{\rm ex} \end{aligned} \tag{S.4}$$

where κ_T is the isothermal compressibility and α_p is the thermal expansivity of the solvent. The average excess energy of hydration, E^{ex}, is the sum the average solute-water interaction energy E_{sw} and E_{reorg}, the reorganization energy. The latter is given by the change in the average potential energy of the solvent in the solute-solvent system minus that in the neat solvent system. (Note that solute-solvent interactions are not counted as part of E_{reorg}.) Ignoring pressure-volume effects, the excess enthalpy of hydration $h^{\text{ex}} = E^{\text{ex}}$. The solute-solvent interaction contribution E_{sw} can be further decomposed into backbone-solvent, E_{bb}, and sidechain-solvent, E_{sc}, contributions. These contributions were straightforwardly obtained using the PairInteraction module within NAMD. The coupled peptide solvent system was simulated for an additional 3 ns and frames were archived every 500 fs for interaction-energy analysis.

For calculating E_{reorg} we adapted the hydration-shell-wise procedure developed earlier [19]. We define an inner-shell around the peptide as the union of shells of radius λ centered on the peptide heavy atoms. $\lambda \leq 5$ Å, $5.0 < \lambda \leq 8$ Å, and $8.0 < \lambda \leq 11.0$ Å defined the first, second, and third shells, respectively. Let n_w be the number of water molecules in a shell for some chosen configuration. The potential energy of the these n_w waters is given by the interaction energy between these n_w waters plus half the interaction energy of these n_w waters with the rest of the fluid. We thus find the average potential energy, $\langle E_{shell} \rangle$, and the average population, $\langle n_{shell} \rangle$, for a given shell. The contribution to the average reorganization energy from the shell is then $\langle E_{shell} \rangle - \langle n_{shell} \rangle \cdot \langle \varepsilon_w \rangle$. Errors are propagated using standard rules. For the antiparallel configuration of helices, we find that by the third shell bulk behavior is attained; that is, $E_{reorg,3} \approx 0$, where $E_{reorg,3}$ is the reorganization energy contribution from the third (3^{rd}) shell. For the parallel configuration, $E_{reorg,3} \approx 5 \pm 2$ kcal/mol and hence this was also included in the calculation. Given the magnitudes and statistical uncertainties, we expect water beyond the third shell will follow bulk behavior.

[1] D. S. Tomar, V. Weber, and D. Asthagiri, Biophys. J. **105**, 1482 (2013).

[2] S. E. Feller, Y. Zhang, R. W. Pastor, and B. R. Brooks, J. Chem. Phys. **103**, 4613 (1995).

[3] J. P. Ryckaert, G. Ciccotti, and H. J. C. Berendsen, J. Comput. Phys. **23**, 327 (1977).

[4] L. Kale, R. Skeel, M. Bhandarkar, R. Brunner, A. Gursoy, N. Krawetz, J. Phillips, A. Shinozaki, K. Varadarajan, and K. Schulten, J. Comput. Phys. **151**, 283 (1999).

[5] V. Weber and D. Asthagiri, J. Chem. Theory Comput. **8**, 3409 (2012).

[6] G. Hummer and A. Szabo, J. Chem. Phys. **105**, 2004 (1996).

[7] R. Friedberg and J. E. Cameron, J. Chem. Phys. **52**, 6049 (1970).

[8] M. P. Allen and D. J. Tildesley, *Computer simulation of liquids* (Oxford University Press, 1987), chap. 6. How to analyze the results, pp. 192–195.

[9] D. M. Rogers and T. L. Beck, J. Chem. Phys. **129**, 134505 (2008).

[10] N. Lu and D. A. Kofke, J. Chem. Phys. **114**, 7303 (2001).

[11] G. Hummer, L. R. Pratt, and A. E. Garcia, J. Phys. Chem. pp. 1206–1215 (1996).

[12] G. Hummer, L. R. Pratt, and A. E. Garcia, J. Phys. Chem. A **102**, 7885 (1998).

[13] W. C. Still, A. Tempczyk, R. C. Hawley, and T. Hendrickson, J. Am. Chem. Soc. **112**, 6127 (1990).

[14] J. Weiser, P. Senkin, and W. C. Still, J. Comp. Chem. **20**, 217 (1999).

[15] A. Onufriev, D. Bashford, and D. A. Case, J. Phys. Chem. B **104**, 3712 (2000).

[16] E. Darve, D. Rodriguez-Gómez, and A. Pohorille, J. Chem. Phys. **128**, 144120 (2008).

[17] J. Hénin, G. Fiorin, C. Chipot, and M. L. Klein, J. Chem. Theory Comput. **6**, 35 (2010).

[18] R. B. Best, X. Zhu, J. Shim, P. E. M. Lopes, J. Mittal, M. Feig, and A. D. MacKerell, Jr., J. Chem. Theory Comput. **8**, 3257 (2012).

[19] D. Asthagiri, S. Merchant, and L. R. Pratt, J. Chem. Phys. **128**, 244512 (2008).

[20] M. E. Paulaitis and L. R. Pratt, Adv. Prot. Chem. **62**, 283 (2002).

[21] T. L. Beck, M. E. Paulaitis, and L. R. Pratt, *The potential distribution theorem and models of molecular solutions* (Cambridge University Press, Cambridge, UK, 2006).

[22] L. R. Pratt and D. Asthagiri, in *Free energy calculations: Theory and applications in chemistry and biology*, edited by C. Chipot and A. Pohorille (Springer, Berlin, DE, 2007), vol. 86 of *Springer series in Chemical Physics*, chap. 9, pp. 323–351.